Focusing of a Rydberg Positronium Beam with an Ellipsoidal Electrostatic Mirror

A. C. L. Jones,* J. Moxom, H. J. Rutbeck-Goldman, K. A. Osorno, G. G. Cecchini, M. Fuentes-Garcia, R. G. Greaves, D. J. Adams, H. W. K. Tom, and A. P. Mills, Jr.
Department of Physics and Astronomy, University of California, Riverside, California 92521, USA

M. Leventhal
Department of Astronomy University of Maryland, College Park, Maryland 20742, USA
(Received 1 January 2017; revised manuscript received 21 April 2017; published 2 August 2017)

Slow atoms in Rydberg states can exhibit specular reflection from a cylindrical surface upon which an azimuthally periodic potential is imposed. We have constructed a concave mirror of this type, in the shape of a truncated oblate ellipsoid of revolution, which has a focal length of (1.50 ± 0.01) m measured optically. When placed near the center of a long vacuum pipe, this structure brings a beam of $n = 32$ positronium (Ps) atoms to a focus on a position sensitive detector at a distance of (6.03 ± 0.03) m from the Ps source. The intensity at the focus implies an overall reflection efficiency of ~30%. The focal spot diameter (32 ± 1) mm full width at half maximum is independent of the atoms' flight times from 20 to 60 μs, thus indicating that the mirror is achromatic to a good approximation. Mirrors based on this principle would be of use in a variety of experiments, allowing for improved collection efficiency and tailored transport or imaging of beams of slow Rydberg atoms and molecules.

DOI: 10.1103/PhysRevLett.119.053201

The large Stark shifts of certain long-lived highly excited (i.e., Rydberg) states of atoms [1] and molecules [2] and the ground states of polar molecules, facilitate their manipulation using inhomogeneous electric fields [3–9]. In particular, a beam of Rydberg H atoms has been shown to reflect from the gradient of the absolute value of a quadrupole electric field [10] and a seeded beam of H has been field decelerated and trapped in an electrostatic multipole trap [11]. More recently, a beam of Rydberg positronium (Ps) atoms [12,13] has been guided using a quadrupole electrostatic field [14], and a beam of metastable Rydberg He atoms has been trapped around a charged wire [15]. The same type of beam has been focused with little distortion using a hexapole electrostatic field [16], which is equivalent to an ordinary positive or convex lens. In this Letter we introduce a new component for atom beam optics by showing that a cylindrical surface with an azimuthally periodic potential can act as a perfect mirror for slow Rydberg atoms. We demonstrate this by focusing a beam of Rydberg Ps using an ellipsoidal azimuthally periodic potential electrostatic mirror. Since the specularly reflecting surface is produced by a short-range repulsive effective potential, mirrors of this type are nearly achromatic. This suggests a number of possibilities for manipulating beams of slow Rydberg atoms in phase space, including tuning their energy, and steering, collecting, and focusing them to diffraction limited spots. For example, the mirror technique described here could find use in the measurement of the Ps trajectories in a precision determination of the 1^3S_1–2^3S_1 interval [17,18], and for increasing the collection efficiency for measurements of the Ps energy of emission from solids [19].

A concave optical quality electrostatic mirror could provide a means for the realization of an experiment for measuring the free fall acceleration of Rydberg Ps or antihydrogen atoms in horizontal flight to test the possibility of antigravity being associated with antimatter [20,21]. Being able to focus antimatter Rydberg atoms with noncontacting mirrors would also be of interest to the scientists working on antihydrogen, for example, the AEGIS [22,23], ALPHA [24], ATRAP [25], and ASACUSA [26] Collaborations. The new mirror could lead to improved ways of controlling and measuring the states of Rydberg atoms [27,28] and polar molecules [7]. A noncontacting periodic potential electrostatic mirror might also be used for producing the gravitational bouncing ball quantum states of positronium [29] or antihydrogen [30].

The basis for the manipulation of Rydberg atoms is the fact that an externally applied electric field $\vec{F}$ causes the states of an atom to exhibit Stark shifts with energies given in the case of Ps by [31]

$$E_{\mathrm{Stark}}(F,n,k,m) = \frac{3}{2} nkea_{0_{\mathrm{Ps}}}|\vec{F}| + \cdots \approx 1.588 \times 10^{-10}\ \mathrm{eV} \times nk|\vec{F}|, \quad (1)$$

which to first order is independent of the magnetic quantum number m. Here, $|\vec{F}|$ is in V/m, n is the principal quantum number, $a_{0_{\mathrm{Ps}}}$ is the Ps Bohr radius, and k is the difference between the parabolic quantum numbers n_1 and n_2 [32] defined in a coordinate system with the electric field along the axis of quantization. The permitted values of k span the range from $-(n - |m| - 1)$ to $+(n - |m| - 1)$ in steps of 2.

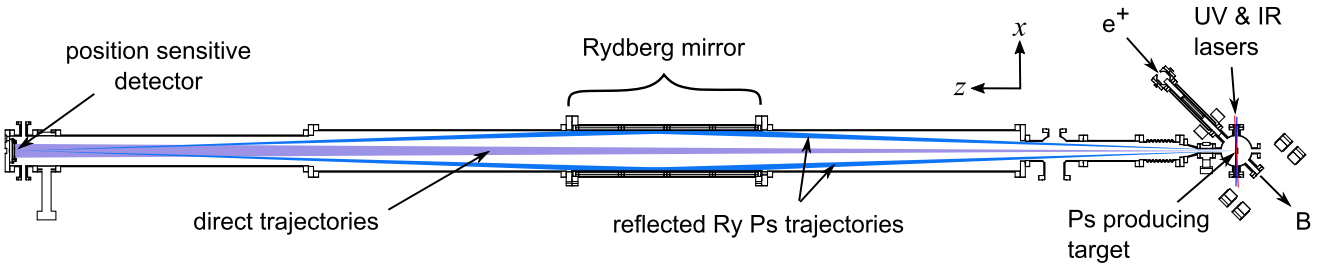

FIG. 1. Schematic of the full 6 m Rydberg atom flight path, with the mirror approximately centered between the Ps producing target (at right) and position sensitive detector. For a more detailed illustration of the target chamber, see Fig. 2(d).

The potential energy of a slowly moving atom, for which the axis of quantization will follow the direction of an external electric field adiabatically [33,34], will be $U(\vec{x}) = E_{\mathrm{Stark}}(\vec{x})$. Suppose we have an infinitely long cylinder of radius R and with its axis along $\hat{z}$, on which is imposed a periodic electrostatic potential $V(R,\theta,z) = V_0 \sin(j\theta)$, where θ is the azimuthal angle and j is an integer $j > 0$. The potential within the cylinder at radius r is $V(r,\theta,z) = V_0(r/R)^j \sin(j\theta)$ and the magnitude of the electric field is $|\vec{F}(r,\theta,z)| = |\vec{\nabla}V(r,\theta,z)| = jV_0(r^{j-1}/R^j)$ with no θ dependence. For $j \gg 1$, a slow Rydberg atom approaching the inner surface of the cylinder experiences a short-range potential that is approximately exponential,

$$U(\rho) \cong 1.588 \times 10^{-10}\ \mathrm{eV} \times nk \frac{V_0}{\rho_0} \exp\left(\frac{-\rho}{\rho_0}\right), \quad (2)$$

where $\rho = R - r$, $\rho_0 = R/(j-1)$ and V_0 and ρ_0 are in units of volts and meters. This potential is only dependent on the distance ρ from the surface. States with positive k will see a sharply rising repulsive potential that may be used as a smooth mirror surface for Rydberg atoms. We note that our discussion above for Rydberg Ps atoms is valid, with a change of energy scale, for any Rydberg atom. While avoided level crossings will limit the maximum kinetic energy of the atoms that can be reflected from a periodic potential mirror, this will not be a significant limitation for atoms with a sufficiently small radial component of velocity.

We now describe our experiment using a 6 m flight path, as illustrated in Fig. 1, and a Rydberg mirror, shown in Figs. 2(a)–2(c), to measure Ps times of flight (TOF) with mirror on and off as plotted in Fig. 3, and the quality of the Rydberg Ps focal spot illustrated in Figs. 4 and 5. We have constructed a periodic potential electrostatic mirror in the form of a wire structure of length 0.9 m and 96 mm mean inside radius in the shape of a truncated oblate ellipsoid of revolution, as shown in Figs. 2(a)–2(c). The mirror is composed of a cylindrical array of 360 stainless steel wires 914 mm long and 1 mm in diameter, with alternating positive and negative potentials. Each wire is supported at the inner edges of one of two sets of 5 electrically isolated stainless steel disks of varying inside radii chosen to give the desired curved inner surface for the array. This structure is mounted coaxially near the center of the 6 m long vacuum pipe illustrated in Fig. 1 with a 1.8 mm FWHM Ps-emitting spot at one end and a position-sensitive microchannel plate (MCP) Rydberg atom detector at the other.

The mirror was tested in air by measuring the image of a 3 mm square white light LED source positioned on the mirror axis at $z = (-3.00 \pm 0.01)$ m from the center of the mirror (at $z = 0$). The light reflected on a paper screen on the other side of the mirror ($z > 0$) was recorded with a CCD camera. The position for obtaining the maximum intensity at the center of the image was $z = (+2.95 \pm 0.05)$ m, in agreement with the mirror's design parameters. The image had an intensity distribution in the image plane

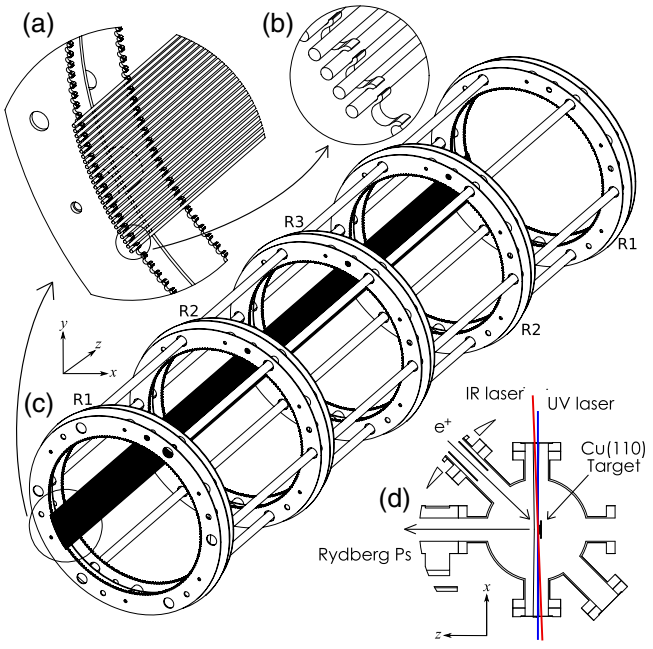

FIG. 2. Schematics of the focusing Rydberg atom mirror and associated experimental apparatus. In (c) the mirror is shown, with a subset of the 360 wires drawn. (a) and (b) Detail of the wire structure and interleaved assembly that defines the periodic potential. (d) Details of the target chamber where Rydberg Ps atoms are prepared. The support rings hold the wires in elliptical arcs, with mean radii of 95.78 at R1, 96.56 at R2, and 96.98 mm at R3.

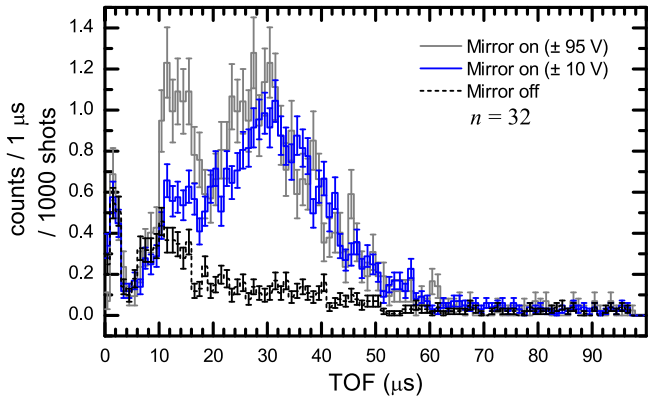

FIG. 3. Data taken with the Rydberg focusing mirror on and off, plotted as a function of Ps TOF with mirror on data collected with applied potentials of ±10 and ±95 V.

[see Fig. 4(c)] that is consistent with a $1/r$ distribution, expected from the superposition of the light reflected from the circular cross section wires composing the mirror, folded with a 2D Gaussian of 21 ± 3 mm FWHM. The larger than expected optical focal spot diameter (which for a perfect lens would be comparable to the ~3 mm diameter of the LED used), is explained by a slight bowing of the 1.0 mm diameter mirror wires with a ~25 μm peak-to-peak amplitude and a period of ~15 cm in addition to a bowing of comparable magnitude due to the gravitational sagging of the wires between the supports. A simulation shows that

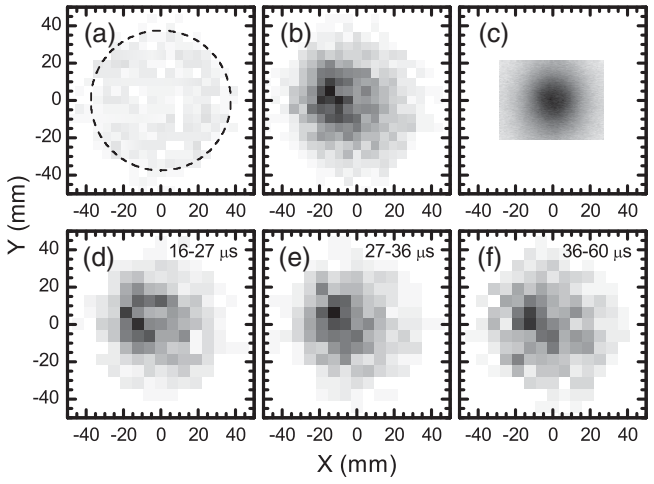

FIG. 4. 2D histograms of the recorded position data of $n = 32$ Rydberg Ps incident upon the detector with (a) the mirror off and (b) the mirror on with ±10 V applied potentials. In (c) the best focus achieved with the mirror using light is shown for comparison. In plots (d)–(f) the data of (b) are subdivided into three velocity groups, for flight times (d) 16–27, (e) 27–36, and (f) 36–80 μs, illustrating that the mirror focus is largely free of chromatic abberations. The dashed circle in (a) indicates the extent of the active area of the MCP. The color scales in plots (b)–(f) represent the total number of counts detected per unit area, and range from white for zero counts to black for the maxmium signal. Plot (a) has the same color scale as plot (b).

for a point source of Rydberg Ps, the higher harmonics of the potential due to its not being exactly equal to $V_0 \sin(j\theta)$ on the mirror surface will result in an intrinsic Rydberg Ps image ~0.5 mm in FWHM for ±10 V mirror potentials.

The position sensitive detector comprises a pair of 75 mm diameter Photonis channel plates (MCPs) in front of a ~25 Ω/square, 90×90 mm^2 indium-tin oxide coated glass resistive anode readout plate. Rydberg atoms are ionized by a 3 mm wide region of electric field ~10^6 V/m between the entrance to the MCP and an 80 mm diameter grounded grid [35] made of parallel 25 μm diameter tungsten wires with 1 mm spacing. Signals from the corners of the anode are amplified and recorded using a LeCroy HDO4054 oscilloscope. The detector was calibrated using UV light and a patterned mask. Pin cushion distortion [36,37] is corrected to first order using the transformation $(x, y) \rightarrow (x/[1 + \alpha y^2], y/[1 + \alpha x^2])$ with $\alpha = 8$ chosen to give an optimally circular image of the active area of the MCP disk [see Fig. 4(a)]. The resolution near the center of the detector is 4.3 ± 1.0 mm FWHM [38].

Positronium for our experiment is formed when 10 ns bursts of 10^5 positrons, accumulated for 1.5 s intervals in a buffer gas trap [39,40] fed by a solid-neon moderated [41] beam of positrons from a ~10 mCi ^{22}Na source, are implanted at 1.5 keV into a single-crystal Cu(110) target [see Fig. 2(d)], held at a temperature of 950 K [42]. Ps emitted from the target is excited to $n = 32$ Rydberg states, as in Ref. [43]. The UV and IR laser beams are directed approximately parallel to the sample surface and near perpendicular

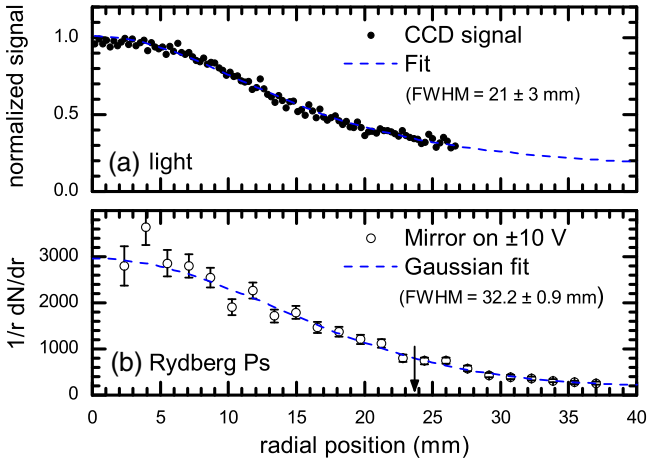

FIG. 5. Radial distributions of the focal spots produced by (a) light and (b) Rydberg Ps. Fits to each data set are also shown, with widths indicated in the legends. The Ps data are that of Fig. 4(b) taken for flight times between 20–80 μs. The vertical arrow in plot (b) indicates the radial distance to the nearest edge of the active area of the MCP, beyond which the distribution may be expected to deviate from the fitted model. The function fitted to the CCD signal in (a) is $1/r$ folded with a 2D Gaussian (see text), the FWHM stated represents that of the Guassian contribution alone.

to the detected Ps flight trajectories [43] to minimize first-order Doppler shifts as illustrated in Fig. 2(d).

The time of flight (TOF) spectra for $n = 32$ Ps traveling from the Cu(110) target to the MCP detector are plotted in Fig. 3 for mirror potentials of ± 95 and ± 10 V ("mirror on") and 0 V ("mirror off"). These data illustrate the signal enhancement resulting from turning on the mirror potentials. A large excess of counts due to the mirror is evident for Ps flight times t in the range of 10 to 60 μs. For $t < 20$ μs the Ps emission is primarily due to spontaneous emission [19,44], while the remaining portion is due to thermal emission [42,45]. The Ps atoms produced through spontaneous emission, which have kinetic energies up to $\sim$1.8 eV, are only efficiently reflected by the mirror with absolute potentials in excess of $\sim$20 V, as seen in the contrast of the two mirror on data sets at flight times $t < 20$ μs. The peak in the signal at $\sim$15 μs also has a large contribution from UV induced background [35]. At long flight times the apparent mirror on-off ratio diminishes, which may result from a combination of effects. Interaction with background thermal radiation [46,47] may excite transitions that randomize the k state [48], thus approximately halving the probability of reflecting. Similarly, spontaneous radiative decay may affect the k state, or simply reduce the observed signal [49]. For flight times greater than 80 μs, the observed signal rate of 2×10^{-5} counts per shot per μs, appears to be a uniform background signal.

A fit to the data over the Lyman-α resonance (not shown) indicates that the mirror increases the count rate by a factor of 6.96 ± 1.17. To maximize the signal rate, the IR wavelength is set to slightly above the Stark fan center, ensuring that the Ps is excited to states of $k > 0$ with maximum possible efficiency.

A direct illustration of the focusing effect of the mirror is shown in Figs. 4(a) and 4(b), which give the two-dimensional distributions of events detected by the MCP with the mirror potentials off (a) and on (b) for $n = 32$ Ps. Although not shown, similar results have also been obtained for $n = 38$ Ps. The data for these measurements are averaged over UV wavelengths between 242.995 and 243.065 nm [50] and TOFs between 20 and 100 μs. To determine the focal width of the spot, the data of Figs. 4(b) and 4(c) and the image of the white light LED source have been binned as a function of radial distance r from the focus center divided by r, to produce the averaged radial distributions plotted in Fig. 5. The Gaussian fit to the Ps data indicates that the spot has a width of 32.2 ± 0.9 mm FWHM. For comparison, the best optical focus, shown in Figs. 4(c) and 5(a) has a Gaussian component with a FWHM of 21 ± 3 mm. The additional broadening observed with Ps is primarily attributed to the small offsets of the mirror (-11 cm) and detector ($+14$ cm) from their ideal relative axial positions, which simulation suggests should produce a $\sim$10 mm diameter ring image at the detector.

The maximum possible ratio of count rates for mirror on versus off would be one plus the ratio of solid angles of the mirror and the MCP detector (18.7:1), yielding an upper limit of $\sim$19.7 here. The observed effect is smaller than this principally due to the inefficiency of the production of focusable Rydberg states in our experiment, owing to the relatively broad bandwidth of the IR laser ($\sim$55 GHz) and the motionally induced Stark shift of Ps in the target chamber. Simulation suggests that the peak production efficiency is $\sim$35%, yielding a predicted signal ratio of 7.5:1, in good agreement with the observed effect of $(7.0 \pm 1.2):1$.

In conclusion, we have demonstrated the effectiveness of a new type of mirror for focusing Rydberg atoms which could be useful for imaging and for tests of the gravitational free fall of antimatter. For the mirror described here, with applied potentials ± 100 V, the reflection of $n = 32$ Rydberg Ps is permitted and is adiabatic for longitudinal velocities up to 9×10^5 m/s or longitudinal kinetic energies of about 4 eV in the highest available k state, limited by ionization in the electric field of the mirror. As pointed out for hydrogen previously [10], since the Rydberg spectrum of hydrogenic atoms has no quantum defect, the full range of the Stark effect for fields up to the ionization limit will be effective in reflecting Rydberg Ps. We find that intersection of the $\sim$5 V/m ambient motional electric field with the fringes of the mirror field should cause only a very small distortion of the focused Ps spot and that a mirror for back reflection should work for Rydberg Ps with thermal energies less than 100 K.

We are grateful to Dr. David B. Cassidy of University College London for helpful suggestions for improving our manuscript. This work was supported in part by the National Science Foundation under Grants No. PHY 1404576 and No. PHY 1505903.

*adric.jones@ucr.edu

[1] T. F. Gallagher, *Rydberg Atoms* (Cambridge University Press, Cambridge, England, 1994).
[2] G. Herzberg, Rydberg molecules, Annu. Rev. Phys. Chem. **38**, 27 (1987).
[3] W. H. Wing, Electrostatic Trapping of Neutral Atomic Particles, Phys. Rev. Lett. **45**, 631 (1980).
[4] T. Breeden and H. Metcalf, Stark Acceleration of Rydberg Atoms in Inhomogeneous Electric Fields, Phys. Rev. Lett. **47**, 1726 (1981).
[5] S. R. Procter, Y. Yamakita, F. Merkt, and T. P. Softley, Controlling the motion of hydrogen molecules, Chem. Phys. Lett. **374**, 667 (2003).
[6] E. Vliegen, H. J. Wörner, T. P. Softley, and F. Merkt, Nonhydrogenic Effects in the Deceleration of Rydberg Atoms in Inhomogeneous Electric Fields, Phys. Rev. Lett. **92**, 033005 (2004).
[7] S. Y. T. van de Meerakker, H. L. Bethlem, N. Vanhaecke, and G. Meijer, Manipulation and control of molecular beams, Chem. Rev. **112**, 4828 (2012).

[8] M. Lemeshko, R. V. Krems, J. M. Doyle, and S. Kais, Manipulation of molecules with electromagnetic fields, Mol. Phys. **111**, 1648 (2013).
[9] S. D. Hogan, Rydberg-Stark deceleration of atoms and molecules, Eur. Phys. J. Tech. Instrum. **3**, 2 (2016).
[10] E. Vliegen and F. Merkt, Normal-Incidence Electrostatic Rydberg Atom Mirror, Phys. Rev. Lett. **97**, 033002 (2006).
[11] S. D. Hogan and F. Merkt, Demonstration of Three-Dimensional Trapping of State-Selected Rydberg Atoms, Phys. Rev. Lett. **100**, 043001 (2008).
[12] K. P. Ziock, R. H. Howell, F. Magnotta, R. A. Failor, and K. M. Jones, First Observation of Resonant Excitation of High-n States in Positronium, Phys. Rev. Lett. **64**, 2366 (1990).
[13] D. B. Cassidy, T. H. Hisakado, H. W. K. Tom, and A. P. Mills, Jr., Efficient Production of Rydberg Positronium, Phys. Rev. Lett. **108**, 043401 (2012).
[14] A. Deller, A. M. Alonso, B. S. Cooper, S. D. Hogan, and D. B. Cassidy, Electrostatically Guided Rydberg Positronium, Phys. Rev. Lett. **117**, 073202 (2016).
[15] H. Ko and S. D. Hogan, High-field-seeking Rydberg atoms orbiting a charged wire, Phys. Rev. A **89**, 053410 (2014).
[16] O. Kritsun, O. Boiko, and H. Metcalf, Focusing Rydberg atoms in an inhomogeneous dc electric field, *Proceedings of the APS Division of Atomic, Molecular and Optical Physics Meeting Abstracts* (2004), http://flux.aps.org/meetings/YR04/DAMOP04/baps/abs/S120023.html.
[17] M. S. Fee, S. Chu, A. P. Mills, Jr., R. J. Chichester, D. M. Zuckerman, E. D. Shaw, and K. Danzmann, Measurement of the positronium 1^3S_1-2^3S_1 interval by continuous-wave two-photon excitation, Phys. Rev. A **48**, 192 (1993).
[18] A. P. Mills, Jr., *Experiments with Dense Low-Energy Positrons and Positronium, Advances in Atomic, Molecular and Optical Physics* (Elsevier, Academic Press, New York, 2016), Vol. 65, Chap. 5, p. 265.
[19] A. C. L. Jones, H. J. Rutbeck-Goldman, T. H. Hisakado, A. M. Piñeiro, H. W. K. Tom, A. P. Mills, Jr., B. Barbiellini, and J. Kuriplach, Angle-Resolved Spectroscopy of Positronium Emission from a Cu(110) Surface, Phys. Rev. Lett. **117**, 216402 (2016).
[20] A. P. Mills, Jr. and M. Leventhal, Can we measure the gravitational free fall of cold Rydberg state positronium? Nucl. Instrum. Methods Phys. Res., Sect. B **192**, 102 (2002).
[21] A. E. Charman (The ALPHA Collaboration), Description and first application of a new technique to measure the gravitational mass of antihydrogen, Nat. Commun. **4**, 1785 (2013).
[22] A. Kellerbauer *et al.*, Proposed antimatter gravity measurement with an antihydrogen beam, Nucl. Instrum. Methods Phys. Res., Sect. B **266**, 351 (2008).
[23] R. Ferragut *et al.*, Antihydrogen physics: Gravitation and spectroscopy in AEgIS, Can. J. Phys. **89**, 17 (2011).
[24] M. Ahmadi *et al.*, Observation of the 1S-2S transition in trapped antihydrogen, Nature (London) **541**, 506 (2017).
[25] G. Gabrielse, R. Kalra, W. S. Kolthammer, R. McConnell, P. Richerme, D. Grzonka, W. Oelert, T. Sefzick, M. Zielinski, D. W. Fitzakerley, M. C. George, E. A. Hessels, C. H. Storry, M. Weel, A. Müllers, and J. Walz, Trapped Antihydrogen in its Ground State, Phys. Rev. Lett. **108**, 113002 (2012).
[26] Y. Enomoto *et al.*, Synthesis of Cold Antihydrogen in a Cusp Trap, Phys. Rev. Lett. **105**, 243401 (2010).
[27] J. Ahn, T. C. Weinacht, and P. H. Bucksbaum, Information storage and retrieval through quantum phase, Science **287**, 463 (2000).
[28] M. Saffman, Quantum computing with atomic qubits and Rydberg interactions: progress and challenges, J. Phys. B **49**, 202001 (2016).
[29] P. Crivelli, V. V. Nesvizhesky, and A. Yu. Voronin, Can we observe the gravitational quantum states of positronium? Adv. High Energy Phys. **2015**, 173572 (2015).
[30] A. Yu Voronin, V. V. Nesvizhevsky, G. Dufour, and S. Reynaud, Quantum ballistic experiment on antihydrogen fall, J. Phys. B **49**, 054001 (2016).
[31] S. D. Hogan, Calculated photoexcitation spectra of positronium Rydberg states, Phys. Rev. A **87**, 063423 (2013).
[32] H. A. Bethe and E. E. Salpeter, *Quantum Mechanics of One- and Two-Electron Atoms* (Plenum, New York, 1957).
[33] M. Born and V. Fock, Beweis des adiabatensatzes, Z. Phys. **51**, 165 (1928).
[34] C. Zener, Non-adiabatic crossing of energy levels, Proc. R. Soc. A **137**, 696 (1932).
[35] A. C. L. Jones, A. M. Piñeiro, E. E. Roeder, H. J. Rutbeck-Goldman, H. W. K. Tom, and A. P. Mills, Jr., Large-area field-ionization detector for the study of Rydberg atoms, Rev. Sci. Instrum. **87**, 113307 (2016).
[36] W. M. Augustyniak, W. L. Brown, and H. P. Lie, A hybrid approach to two dimensional charged particle position sensing preserving energy resolution, IEEE Trans. Nucl. Sci. **19**, 196 (1972).
[37] M. Lampton and C. W. Carlson, Low-distortion resistive anodes for two-dimensional position-sensitive MCP systems, Rev. Sci. Instrum. **50**, 1093 (1979).
[38] The mean amplitude of the signals from the UV light shining on the MCP surface are known to be about 20% of the mean amplitude of the signals from Rydberg Ps atoms which are field ionized, with the freed positrons subsequently accelerated into the MCP with ~2.5 keV of kinetic energy [35]. Because of this the positional resolution for Rydberg Ps is probably about 2 mm FWHM, although we have not verified this directly.
[39] T. J. Murphy and C. M. Surko, Positron trapping in an electrostatic well by inelastic collisions with nitrogen molecules, Phys. Rev. A **46**, 5696 (1992).
[40] D. B. Cassidy, S. H. M. Deng, R. G. Greaves, and A. P. Mills, Jr., Accumulator for the production of intense positron pulses, Rev. Sci. Instrum. **77**, 073106 (2006).
[41] A. P. Mills, Jr. and E. M. Gullikson, Solid neon moderator for producing slow positrons, Appl. Phys. Lett. **49**, 1121 (1986).
[42] A. P. Mills, Jr. and L. Pfeiffer, Desorption of Surface Positrons: A Source of Free Positronium at Thermal Velocities, Phys. Rev. Lett. **43**, 1961 (1979).
[43] A. C. L. Jones, T. H. Hisakado, H. J. Goldman, H. W. K. Tom, and A. P. Mills, Jr., Polarization dependence of $n = 2$ positronium transition rates to Stark-split $n = 30$ levels via crossed-beam spectroscopy, J. Phys. B **49**, 064006 (2016).

[44] A. P. Mills, Jr., L. Pfeiffer, and P. M. Platzman, Positronium Velocity Spectroscopy of the Electronic Density of States at a Metal Surface, Phys. Rev. Lett. **51**, 1085 (1983).

[45] K. G. Lynn, Observation of Surface Traps and Vacancy Trapping with Slow Positrons, Phys. Rev. Lett. **43**, 391 (1979).

[46] D. H. Menzel, Oscillator strengths for high-level transitions in hydrogen, Nature (London) **218**, 756 (1968).

[47] J. W. Farley and W. H. Wing, Accurate calculation of dynamic Stark shifts and depopulation rates of Rydberg energy levels induced by blackbody radiation. Hydrogen, helium, and alkali-metal atoms, Phys. Rev. A **23**, 2397 (1981).

[48] C. B. Tarter, Coefficients connecting the Stark and field-free wave functions for hydrogen, J. Math. Phys. (N.Y.) **11**, 3192 (1970).

[49] A. Deller, A. M. Alonso, B. S. Cooper, S. D. Hogan, and D. B. Cassidy, Measurement of Rydberg positronium fluorescence lifetimes, Phys. Rev. A **93**, 062513 (2016).

[50] We note that this range is not centered precisely about the $1S$-$2P$ resonance. A 0.01 nm shift is observed, which is probably due to a misalignment of the laser with respect to the mean of the Ps trajectories of 1.6° from perpendicular.